An Economic Model Predictive Control Framework for Mechanical Pulping Processes

Hui Tian[a,1], Qiugang Lu[a], R. Bhushan Gopaluni[a], Victor M. Zavala[b], James A. Olson[c]

[a] *Department of Chemical and Biological Engineering, The University of British Columbia, Vancouver, BC, Canada, V6T 1Z4*
[b] *Department of Chemical and Biological Engineering, The University of Wisconsin-Madison, Madison, WI, USA, 53706*
[c] *Department of Mechanical Engineering and the Pulp and Paper Center, The University of British Columbia, Vancouver, BC, Canada, V6T 1Z4*

Abstract

We develop a multi-objective economic model predictive control (*m-econ* MPC) framework to control and optimize a nonlinear mechanical pulping (MP) process. *M-econ* MPC interprets economic MPC as a multi-objective optimization problem that trades off economic and set-point tracking performance. This interpretation allows us to construct a stabilizing constraint that guarantees closed-loop stability. The framework infers unmeasured states of the MP process (associated with product consistency) by using a moving horizon estimator (MHE). The MP process dynamics are described by using a nonlinear Wiener model. Examples from a two-stage high-consistency MP process are employed to demonstrate that significant improvements in economic performance are achievable.

Keywords: Economic model predictive control; moving horizon estimation; mechanical pulping process; stability

1. Introduction

The mechanical pulping (MP) process is one of the most energy-intensive operations in the pulp and paper industry [1, 2, 3, 4, 5, 6]. The development of control strategies for MP processes dates back to the mid-1970s [2, 3, 4]. Significant research progress has been reported in the fields such as refining optimization, energy reduction, and pulp quality improvement [5, 6, 7, 8]. In recent years, strong global competition has driven the development of new control and optimization techniques to reduce energy consumption and enforce strict pulp quality specifications [9, 10, 11]. The development of advanced control strategies is difficult because MP processes are inherently multivariable and involve strong interactions.

Model predictive control (MPC) is an optimization-based control technique that computes optimal control policies by solving a finite horizon optimization problem in real time. An outstanding feature of MPC is that physical constraints on actuators and outputs can be incorporated directly in the optimization problem. As a result, MPC has attracted considerable research efforts and has been widely applied in various industrial processes [12, 13, 14]. In the context of MP processes, implementations of linear MPC have been reported

[1] Corresponding author. Telephone: +1-604-726-8908; email: huitian@chbe.ubc.ca

in the past decade. These implementations use a linearization of the MP process [3, 15], which results in suboptimal performance due to the presence of strong nonlinearities. The development of advanced optimization algorithms and computing hardware enable the direct handling of nonlinear dynamics in MPC formulations [16, 17, 18, 19]. The authors in [9, 10, 11] presented results on the control and optimization of MP processes using nonlinear MPC (NMPC). In our previous work [20], we proposed a multi-objective economic MPC strategy (that we call *m-econ* MPC) for two-stage high consistency (HC) refining processes [2]. We show that *m-econ* MPC can simultaneously minimize economic cost while enforcing set-point tracking (which is critical to maintain product quality). The controller sees economic and tracking performance as conflicting goals and this insight is used to derive a stabilizing constraint that guarantees closed-loop stability. More recently, the authors in [21] analyzed the inherent robustness properties for an economic NMPC controller, which provides a high flexibility to optimize economic performance and remains robust in the face of disturbances. Despite these advances, extensive obstacles still prevent the deployment of NMPC in MP processes [10]. Among these obstacles, state estimation is of primary importance because many process variables cannot be measured reliably.

The majority of existing work on advanced control for MP processes is based on the assumption that the state variables are measurable and known in real-time. However, information on important variables such as pulp consistency in HC refining is rarely available due to the lack of measurement sensors (particularly fast and reliable online sensors). For instance, one of the most widely used sensors in industry is the pulp quality monitor (PQM) that can measure the shives, fiber size distribution, and freeness in the pulp. This sensor takes measurements infrequently (every 50-60 minutes) and thus limits the use of MPC.

State estimation for nonlinear systems is particularly challenging when there are constraints on the state variables and disturbances [22, 23, 24]. To address such issues, moving horizon estimation (MHE) has been proposed as a practical approach that can directly embed nonlinear dynamics and constraints [25, 26]. In MHE, estimates of the states are obtained in real-time by solving a short horizon optimization problem that minimizes the difference between measurements and predicted outputs. A moving window of fixed size slides forward in time and prior information on estimated states is updated via the so-called arrival cost .

In this paper we develop an economic MPC framework for a two-stage HC refining process that combines *m-econ* MPC with a MHE estimator. Using simulation experiments on a two-stage HC refining process, we demonstrate that state variables can be inferred reliably from limited measurement data and that the MPC can achieve significant improvements in economic performance.

The paper is outlined as follows. In Section 2, we present a brief introduction on the two-stage HC refining process and some preliminaries on the MHE. Section 3 is devoted to the *m-econ* MPC technique for the two-stage HC MP process. The combination of MHE and *m-econ* MPC is elaborated in Section 4. In

[2]The pulp consistency is defined as the mass percentage ratio of wood to the mixture of wood and water. It is high consistency (HC) when this ratio is between 20% and 50%, and it is low consistency (LC) when this value is between 3% and 5%.

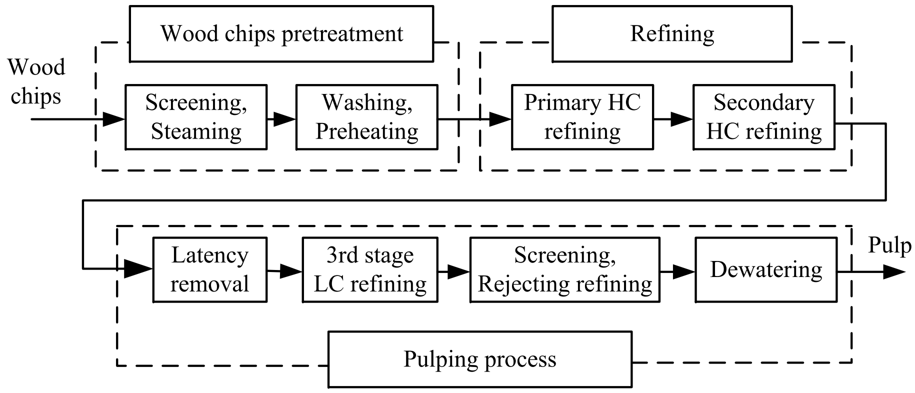

Figure 1: Operational units in a typical two-stage MP process

this section, we also present two simulations to demonstrate the performance of the proposed *m-econ* MPC technique and MHE estimation, followed by conclusions in Section 5.

2. High Consistency Refining Process

2.1. Process description

A multi-stage MP process generally consists of wood chip pretreatment, wood chip refining and pulp refining stages as shown in Figure 1. In the wood chip pretreatment stage, wood chips will be screened to remove over and under sized particles and then steamed and preheated at atmospheric pressure around 100°C. There are typically two high consistency refiners in the wood chip refining stage - a primary and a secondary refiner as shown in Figure 2. After pretreatment, the wood chips are introduced into the inlet of the primary HC refiner by the cylindrical chip transfer screw feeder. Dilution water is usually fed into the inlet of the refiner to control the consistencies in the refining zone. The wood chips are broken down into fibers as they pass through the two rotating discs of the refiners.

The key variables required for control and optimization of the process, such as manipulated variables, operating variables and pulp quality variables, will be discussed in detail in the following subsections.

Main process manipulated variables

Manipulated variables are the input variables which can be adjusted during the process operation. The main inputs in a MP process, shown in Figure 2, are summarized in the left column of Table 1.

(1) Chip transfer screw speed, u_1. The chip transfer screw speed for the primary refiner is the main manipulated variable used to control the flow of chips from the preheater at the wood chips pretreatment stage to the inlet of the primary refiner. Any changes in the screw speed can affect the flow of dry fibres to the refiner. Most pulp mills also use the transfer screw speed to set the desired production rate.

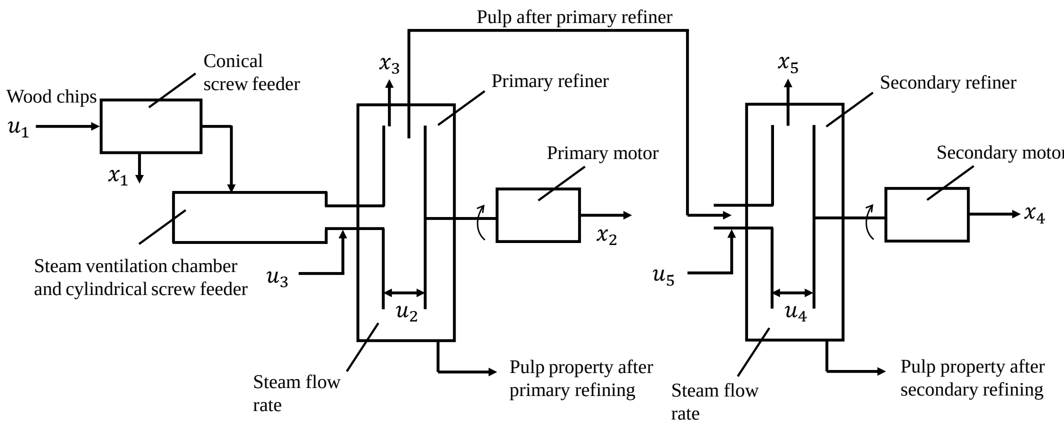

Figure 2: Schematic of two-stage HC refining

Table 1: A list of process variables

MV	Note	Unit	Notation	SV	Note	Unit	Notation
u_1	Chip transfer screw speed	rpm	R	x_1	Production rate	tonnes/day	P
u_2	Primary refiner plate gap	mm	G_p	x_2	Primary motor load	MW	M_p
u_3	Primary dilution flow rate	kg/s	D_p	x_3	Primary consistency ($\star$)	%	C_p
u_4	Secondary refiner plate gap	mm	G_s	x_4	Secondary motor load	MW	M_s
u_5	Secondary dilution flow rate	kg/s	D_s	x_5	Secondary consistency ($\star$)	%	C_s

Note: The variables with ($\star$) are unmeasurable state variables.

(2) Primary/secondary refiner plate gap u_2, u_4. The plate gap is the distance between two plates of a refiner. It is normally controlled by a mechanical loading system. The gap size can be measured by a gap sensor or indicated by changes in the relative shaft position. Variations in gap size directly impact the mechanical force exerted by plates onto wood chips, and thus affect the motor load.

(3) Primary/secondary dilution flow rate u_3, u_5. The refining zone consistency has a major effect on pulp properties. The water added to the refiner will alter the consistency and thus change the pulp quality. Large variations in the dilution water flow rate can also lead to unstable refining operation. Manipulating the water flow rate at the inlet of the each refiner is commonly used by pulp mills to maintain the consistency in refiners.

Main process state/operating variables

The state variables are the key variables and highly correlated with the pulp properties. By controlling manipulated variables the states are maintained at optimum set-points. The optimum set-points in a MPC controller are determined by the economical operation of the MP process. The main process state variables used in this work are summarized in the right column of Table 1.

(1) Production rate x_1. Production rate is one of the most important operating considerations in pulp mills. The production rate can be changed by adjusting the chip transfer screw speed. However, the production rate varies with the variations in the raw wood chip quality such as wood species, chip density, and moisture content. The production rate can also affect the specific energy and the pulp quality.

(2) Primary/secondary motor load x_2, x_4. Among the operating variables, motor load is one of the most important measurements which are highly correlated with the pulp qualities. One way to set and maintain the motor load is to adjust the plate gap since motor load is directly affected by and sensitive to the gap size.

(3) Primary/secondary consistency x_3, x_5. At a given specific energy, the consistency in the refining zone for both the primary and secondary refiners has a major influence on pulp properties. An improved consistency control can significantly reduce the fluctuations of motor load and enhance the refiner performance.

Steam production is also an important operating variable because it is associated with high energy consumption. However, as is common practice in most pulp mills, this variable is rarely considered in control design for MP processes.

Specific energy

Specific energy (SE) (in MW/tonnes/day) is the energy consumed per ton of dry pulp and is a critical variable that strongly affects pulp properties [5]. SE is defined as the ratio of the motor load with respect to the production rate. Therefore, motor load and production rate can be adjusted according to the desired SE. One of the traditional pulp quality control strategies is to manipulate SE based on the quality-energy relationship. For the i-th refiner and motor, SE_i is defined as follows:

$$\text{Specific Energy } (SE_i) := \frac{\text{Motor load}_i}{\text{Production rate}}, \quad i = p, s. \tag{1}$$

where the subscript index $i = p, s$ represents the primary and secondary refiners, respectively. For a two-stage HC MP process, the total SE at time instant t for both primary and secondary refiner is defined as,

$$\text{Total Specific Energy } (TSE_t) := \frac{\text{Total motor load}}{\text{Production rate}}. \tag{2}$$

In our economic MPC design, TSE_t is embedded directly in the objective function and is used as an indicator of economic performance.

Pulp properties

The final pulp quality can be characterized by many property variables such as freeness, fibre length, shive content, coarseness, and strength. To assess the quality of the pulp, we consider the following commonly used pulp properties: Canadian Standard Freeness (CSF, ml), long fibre content (LFC, %) and shive content (SC, %).

Process disturbances

Wood chips are the main raw materials for pulp production and thus variations in wood chips comprise the main disturbance that affect the refining conditions and final pulp properties. In this work, variations existing in the raw chips (such as the chip bulk density and chip moisture content) will be considered as disturbances.

Unmeasurable state variables

The consistency in the primary and secondary refiners (x_3 and x_5) cannot be measured reliably in real-time and thus need to be inferred from the measured outputs (x_1, x_2, and x_4) and inputs ($u_1, \cdots, u_5$). The consistency in the refiner is known to significantly impact pulp properties. A variety of advanced control strategies have been proposed in the literature with the assumption that the consistency can be measured accurately and that it can be used directly by the controller. However, such assumption becomes questionable given that practical sensors are usually not fast enough to measure the consistency in real-time. As a result, a reliable state estimation mechanism for the consistency is needed to reduce fluctuations in the motor load and for stabilizing the MP process.

2.2. HC refining model

The mathematical models of mechanical refining process have been reported recently in [9, 10, 11, 20, 27]. The model used in this paper will be based on the Wiener-type models derived in our previous work [20, 27], which were developed by using a combination of mechanistic and empirical methods. The production rate, motor loads and consistencies for both primary and secondary refiners are treated as discretized differential state variables. The chip-transfer screw speed, plate gap, and dilution water flow rates of each refiner are taken as manipulated variables. The model and disturbances are based on the data collected in identification experiments on actual industrial processes, and it is shown that the developed model can represent the real process with high-fidelity.

Consider the two-stage HC pulping process which can be described by nonlinear difference equations with additive state and measurement noise [3]:

$$x_{t+1} = \underbrace{Ax_t + h(x_t, u_t)}_{f(x_t,u_t)} + \zeta_t, \tag{3}$$

$$y_t = g(x_t) + \eta_t, \tag{4}$$

where $A \in \mathbb{R}^{n_x \times n_x}$ is the dynamic matrix which can be identified for the MP process by using linear system identification methods. $x_t \in \mathbb{R}^{n_x}$, $u_t \in \mathbb{R}^{n_u}$, and $y_t \in \mathbb{R}^{n_y}$ are the states, manipulated variables, and controlled outputs, respectively. For a two-stage HC process, x_t and u_t are defined in Table 1. The state and input variables are required to satisfy the constraints $x_t \in \mathbb{X}$ and $u_t \in \mathbb{U}$, where the sets $\mathbb{X} \subseteq \mathbb{R}^{n_x}$

[3] Please refer to Appendix A for the details of two-stage HC MP process model.

and $\mathbb{U} \subseteq \mathbb{R}^{n_u}$ are compact and contain the equilibrium point (x_{ss}, u_{ss}). The vector $\zeta_t \subseteq \mathbb{R}^{n_\zeta}$ is an additive disturbance affecting the system dynamics and can be used to represent the disturbance attributed to the state transition from x_t to x_{t+1}. The system states can be observed through the measurement equation (4) where $y_t \subseteq \mathbb{R}^{n_y}$ is the observation and $\eta_t \subseteq \mathbb{R}^{n_v}$ is the measurement error. In this work, we assume that η_t is independent and identically distributed (i.i.d.) with known mean and variance. $h(\cdot) : \mathbb{R}^{n_x} \times \mathbb{R}^{n_u} \mapsto \mathbb{R}^{n_x}$ is a nonlinear state function. $f(\cdot) : \mathbb{R}^{n_x} \times \mathbb{R}^{n_u} \mapsto \mathbb{R}^{n_x}$ is a nonlinear function which represents the dynamics that map the current input and state to the state at the next time instant.

The measurement vector y_t is defined as

$$y_t = \left[\check{P}, \check{M}_p, \check{M}_s\right]. \tag{5}$$

where $\check{P}$, $\check{M}_p$, $\check{M}_s$ are the noisy measurements of the state variables P, M_p, M_s, respectively.

2.3. State estimation

For effective control an MPC on the HC refiner has to account for changes in state variables and therefore states have to be estimated to solve the related optimization problem. However, when unmeasurable states are present, the unmeasured states need to be inferred from the available (mostly noisy) measurements. The model (3)–(4) is corrupted with process and measurement noise ζ_t and η_t that are assumed to be normally distributed with zero mean and constant covariance P_ζ and P_η:

$$\zeta_t \sim N(0, P_\zeta), \quad \eta_t \sim N(0, P_\eta). \tag{6}$$

The states of the system need to be inferred from the measured outputs (5). Specifically, MHE uses a moving measurement window of the form:

$$I_t^T = [I_t^{y^T}, I_t^{u^T}] = [y_{t-N_{mhe}}, \cdots, y_{t-1}, y_t, u_{t-N_{mhe}}, \cdots, u_{t-1}], \quad t \geq 0, \tag{7}$$

to compute the estimates $\hat{x}_t$ of the states x_t. N_{mhe} is the size of the moving window for the estimator. I_t is the information vector at time t. We formulate the estimation problem as the solution to the following optimization problem,

$$\min_{z_0, \{\zeta_k\}_{k=0}^{N_{mhe}-1}} \quad J_{mhe} := \mu||z_0 - \bar{x}^0_{t-N_{mhe}}||^2 + \sum_{k=0}^{N_{mhe}} ||y_{t-N_{mhe}+k} - g(z_k)||^2_{Q_\eta} + \sum_{k=0}^{N_{mhe}} ||\zeta_{t-N_{mhe}+k}||^2_{Q_\zeta} \tag{8}$$

$$s.t. \quad z_{k+1} = f(z_k, u_{t-N_{mhe}+k}) + \zeta_k, \quad k = 0, \ldots, N_{mhe} - 1, \tag{9}$$

$$y_k = g(z_k) + \eta_k, \quad k = 0, \ldots, N_{mhe}, \tag{10}$$

$$z_k \in \mathbb{X}, \quad z_{N_{mhe}} \in \mathbb{X}_f, \quad k = 0, \ldots, N_{mhe} - 1, \tag{11}$$

where J_{mhe} is the optimal cost which incorporates the arrival cost (the first term in (8)) and the least-square error of the outputs (the second term in (8)) in the estimation horizon N_{mhe}. $\bar{x}^0_{t-N_{mhe}}$ is the prior value of the initial state and μ is a weighting factor for the arrival cost. The state variables are subject to the state model in (9) as well as the constraints in (11). The solution of the optimization problem is given by the state trajectory $[\tilde{z}_0, \cdots, \tilde{z}_{N_{mhe}}]$. From the solution, we obtain the estimate of the current state of the system as $\hat{x}_t \leftarrow z_{N_{mhe}}$. Conditions for stability of MHE have been established for general settings in [23, 24, 25, 26, 28].

3. *M-econ* MPC for the MP Process

In this section, we focus on the development of *m-econ* MPC for two-stage HC processes.

3.1. Basic notation and setting

Given the model of the two-stage HC refining process in the form (3) − (4), the set-point tracking value function V_t^{tr} and the economic value function V_t^{ec} at time t are given by:

$$V_t^{tr} := \sum_{k=t}^{t+N_{mpc}-1} L^{tr}(\hat{x}_k - x_{ss}, u_k - u_{ss}), \tag{12}$$

$$V_t^{ec} := \sum_{k=t}^{t+N_{mpc}-1} L^{ec}(\hat{x}_k, u_k), \tag{13}$$

where N_{mpc} is the prediction horizon and $\hat{x}_k$ denotes the estimated state at time k from MHE. $L^{tr}(\cdot)$ and $L^{ec}(\cdot)$ are the tracking stage cost and economic stage cost, respectively. (x_{ss}, u_{ss}) are equilibrium points which can be calculated by solving a steady-state optimization problem. The mapping $L^{tr} : \mathbb{R}^{n_x} \times \mathbb{R}^{n_u} \mapsto \mathbb{R}$ is always nonnegative. In the rest of this paper, $L^{tr}(\hat{x}_k, u_k)$ will be used as a compact representation of the stage cost $L^{tr}(\hat{x}_k - x_{ss}, u_k - u_{ss})$. In the formulation of economic MPC, the economic stage cost $L^{ec} : \mathbb{R}^{n_x} \times \mathbb{R}^{n_u} \mapsto \mathbb{R}$ is assumed to be bounded and related directly to the desired economics. The notation $\{\hat{x}_k, u_k\}_t^{t+N_{mpc}}$ will be used hereafter to describe the trajectory of estimated states $\hat{x}_k$, $k = t, \ldots, t + N_{mpc}$, from MHE and the sequence of manipulated variables u_k, $k = t, \ldots, t + N_{mpc} - 1$, for brevity.

In what follows, we assume that the tracking MPC (*tr* MPC) is feasible for any $x_t \in \mathbb{X}$. The optimal trajectory at time $t+1$ is defined as $\{\bar{x}_{k|t+1}, \bar{u}_{k|t+1}\}_{t+1}^{t+1+N_{mpc}}$ and is obtained by solving the optimization problem,

$$\begin{aligned} \min_{v_k} \quad & \sum_{k=0}^{N_{mpc}-1} L^{tr}(z_k, v_k), \\ s.t. \quad & z_0 = \hat{x}_{t+1}, \quad z_{N_{mpc}} \in \mathbb{X}_f, \\ & z_{k+1} = f(z_k, v_k), \quad k = 0, \ldots, N_{mpc} - 1, \\ & y_k = g(z_k), \quad k = 0, \ldots, N_{mpc}, \\ & z_k \in \mathbb{X}, \quad v_k \in \mathbb{U}, \quad k = 0, \ldots, N_{mpc} - 1, \end{aligned} \tag{14}$$

where z_k, v_k are the internal optimization variables representing states and controls, respectively. For the nonlinear MP process defined in (3)-(4), we require that the terminal states lie in the terminal region $\mathbb{X}_f$ instead of at the desired steady state x_{ss}. $\mathbb{X}_f \in \mathbb{X}$ is a compact terminal region containing a neighborhood of the point x_{ss} in its interior. The value function for *tr* MPC at time $t+1$ is shown to be

$$\bar{V}_{t+1}^{tr} := \sum_{k=t+1}^{t+N_{mpc}} L^{tr}(\bar{x}_{k|t+1}, \bar{u}_{k|t+1}). \tag{15}$$

In the standard *tr* MPC problem, the stage cost is normally defined as penalizing the deviation of process variables from their steady-state values. The closed-loop stability of *tr* MPC is established by treating the optimal cost along the closed-loop trajectory as a Lyapunov function [29, 30, 31, 32]. However, for economic MPC, the corresponding stage cost function is defined by $L^{ec}(\cdot)$, which may be selected by the user according to practical needs and such function may not be positive definite. As a result, most practical economic cost functions cannot be used as Lyapunov functions and closed-loop stability cannot be guaranteed. In the next subsection, we combine *tr* MPC and economic MPC into the multi-objective MPC formulation to enforce stability.

3.2. Multi-objective economic MPC

The trajectory $\{\bar{x}_{k|t+1}, \bar{u}_{k|t+1}\}_{t+1}^{t+1+N_{mpc}}$ is optimal for the standard *tr* MPC problem in (14). Stability of standard *tr* MPC technique is achieved by treating the tracking stage cost L^{tr} as a Lyapunov function. Specifically, from Lyapunov theory for standard *tr* MPC, a sufficient condition that ensures closed-loop stability is [32]:

$$\bar{V}_{t+1}^{tr} - V_t^{tr} \leq -L^{tr}(x_t, u_t). \tag{16}$$

A less restrictive condition, reported in [33], shows that stability of *any* alternative MPC formulation can also be guaranteed if the associated trajectory $\{x_{k|t+1}, u_{k|t+1}\}_{t+1}^{t+1+N_{mpc}}$ satisfies:

$$V_{t+1}^{tr} \leq \bar{V}_{t+1}^{tr} + \sigma(V_t^{tr} - \bar{V}_{t+1}^{tr}), \tag{17}$$

where $\sigma \in [0, 1)$ is a scalar. Here, $\bar{V}_{t+1}^{tr}$ (defined in (15)) is the value function of the optimal trajectory for the tracking MPC at time instant $t+1$. The actual value function V_{t+1}^{tr} in (17) is defined as:

$$V_{t+1}^{tr} := \sum_{k=t+1}^{t+N_{mpc}} L^{tr}(x_{k|t+1}, u_{k|t+1}). \tag{18}$$

Since any feasible trajectory satisfying (17) leads to closed-loop stability, we may impose this condition as a *stabilizing constraint* when formulating an economic MPC controller, which results in the *m-econ* MPC formulation:

$$\begin{aligned}
\min_{v_k} \quad & \sum_{k=0}^{N_{mpc}-1} L^{ec}(z_k, v_k), && (19)\\
s.t. \quad & z_0 = \hat{x}_{t+1}, \quad z_{N_{mpc}} \in \mathbb{X}_f, \\
& z_{k+1} = f(z_k, v_k), \quad k = 0, \ldots, N_{mpc}-1, \\
& y_k = g(z_k), \quad k = 0, \ldots, N_{mpc}, \\
& z_k \in \mathbb{X}, v_k \in \mathbb{U}, \quad k = 0, \ldots, N_{mpc}-1, \\
& \sum_{k=0}^{N_{mpc}-1} L^{tr}(z_k, v_k) \leq \epsilon_{t+1}(\sigma), \quad k = 0, \ldots, N_{mpc}-1, && (20)
\end{aligned}$$

where

$$\epsilon_{t+1}(\sigma) := \bar{V}_{t+1}^{tr} + \sigma(V_t^{tr} - \bar{V}_{t+1}^{tr}). \tag{21}$$

Note that the constraint in (20) is equivalent to the stabilizing constraint (17). Closed-loop stability of *m-econ* MPC is then guaranteed by the stabilizing constraint in (17). The argument of this statement is outlined as follows. Adding the term $-V_t^{tr}$ to both sides of (17) we have

$$V_{t+1}^{tr} - V_t^{tr} \leq (1-\sigma)(\bar{V}_{t+1}^{tr} - V_t^{tr}). \tag{22}$$

Combining (17) and (22), the following inequality holds for any feasible solution,

$$V_{t+1}^{tr} - V_t^{tr} \leq -(1-\sigma)L^{tr}(x_t, u_t). \tag{23}$$

Since $(1-\sigma)L^{tr}(x_t, u_t)$ is nonnegative for $\sigma \in [0, 1)$, we can conclude that the trajectory $\{x_{k|t+1}, u_{k|t+1}\}_{t+1}^{t+1+N_{mpc}}$ obtained from solving the *m-econ* MPC algorithm (19)–(21) is stable. More precisely, the closed-loop system is asymptotically stable under the control law obtained from solving the *m-econ* MPC problem for any $\sigma \in [0, 1)$. A detailed derivation of this result is provided in [33].

Remark 1. Note that by imposing the stabilizing constraint (17) to the *m-econ* MPC, we can merge the capability of *tr* MPC in assuring closed-loop stability and the merits of economic MPC together to achieve both tracking and economic performances. Although we may sacrifice certain economic profit compared with the pure economic MPC, what we gain in guaranteeing the stability is much more meaningful and crucial for most practical MP processes. Moreover, this *m-econ* MPC method provides a degree-of-freedom (the tuning parameter σ) to tune the trade-off between economics and tracking performance.

4. *M-econ* MPC and MHE Design for the MP Process and Simulation Results

4.1. M-econ MPC and MHE Design for the MP Process

The MP process is a complex multi-input multi-output (MIMO) nonlinear process with strong interactions among variables. Based on the two-stage HC model developed in (3)-(4) and the *m-econ* MPC and MHE approaches presented in the previous section, we are now in a position to combine the MHE and *m-econ* MPC for MP processes. The graphical depiction of the integrated *m-econ* MPC and MHE framework is shown in Figure 3.

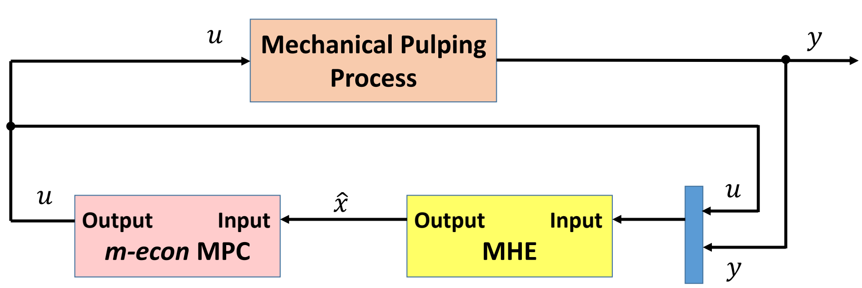

Figure 3: Graphical depiction of the integrated *m-econ* MPC and MHE for MP process

Table 2: The implementation of *m-econ* MPC and MHE for a two-stage HC process

Algorithm of the *m-econ* MPC and MHE	
Input:	$x_0 \in \mathbb{X}$, $\sigma \in [0,1)$, set $t \leftarrow 0$ and $\epsilon_0(\sigma) \leftarrow +\infty$.
Loop:	**for** $t = 0, \ldots, T$ (simulation ends) **do**
1:	Solve the *m-econ* MPC optimization in (24)-(29) for the state x_t and $\epsilon_t(\sigma)$, evaluate V_t^{tr}, and set $u_t \leftarrow v_0$.
2:	Implement u_t to the plant and obtain the state variables $x_{t+1} = f(x_t, u_t) + \zeta_t$.
3:	Solve *tr* MPC in (14) for the state x_{t+1}, and evaluate $\bar{V}_{t+1}^{tr}$.
5:	Solve MHE in (8)-(11) to get the estimates $[\tilde{z}_0, \cdots, \tilde{z}_{N_{mhe}}]$.
6:	Set $\epsilon_{t+1}(\sigma) \leftarrow \bar{V}_{t+1}^{tr} + \sigma(V_t^{tr} - \bar{V}_{t+1}^{tr})$ and $x_{t+1} \leftarrow \tilde{z}_{N_{mhe}}$.
7:	**end loop**

For the specific MP process considered in this work, the tracking and economic objective functions are defined as

$$\begin{aligned} V_t^{tr} &= \sum_{k=t}^{t+N_{mpc}-1} ||\hat{x}_k - x_{ss}||_{Q_x}^2 + ||u_k - u_{ss}||_{Q_u}^2, \\ V_t^{ec} &= \sum_{k=t}^{t+N_{mpc}-1} TSE_k, \end{aligned}$$

where N_{mpc} is the prediction horizon and Q_x, Q_u are positive-definite weighting matrices for the state and input variables, respectively. TSE_k is the total energy as defined in (2) and given by $([0,1,0,0]\ \hat{x}_k + [0,0,0,1]\ \hat{x}_k)\ /\ [1,0,0,0]\ \hat{x}_k$ for the specific MP process under study. The *m-econ* MPC optimization problem for the MP process can be formulated as follows,

$$\min_{v_k} \sum_{k=t}^{t+N_{mpc}-1} TSE_k, \tag{24}$$

$$s.t. \quad z_0 = \hat{x}_{t+1},\ z_{N_{mpc}} \in \mathbb{X}_f, \tag{25}$$

$$z_{k+1} = f(z_k, v_k), \quad k = 0, \ldots, N_{mpc}, \tag{26}$$

$$x_{min} \leq z_k \leq x_{max}, \quad k = 0, \ldots, N_{mpc}, \tag{27}$$

$$u_{min} \leq v_k \leq u_{max}, \quad k = 0, \ldots, N_{mpc} - 1, \tag{28}$$

$$\sum_{k=t}^{t+N_{mpc}-1} ||z_k - x_{ss}||_{Q_x}^2 + ||v_k - u_{ss}||_{Q_u}^2 \leq \epsilon_{t+1}(\sigma), \tag{29}$$

where $\sigma \in [0,1)$ and $\epsilon_{t+1}(\sigma)$ is defined in (21). Here, we note that the stabilizing constraint takes the form of a ball centered around the equilibrium point (x_{ss}, u_{ss}) and with radius $\epsilon_{t+1}(\sigma)$. Consequently, the stabilizing constraint can be interpreted as a *trust-region* that the MPC controller can visit to optimize economics while preserving stability.

At each time instant, the optimal input sequence can be obtained by solving the *m-econ* MPC (24)–(29) [4]. Only the first input of the optimal input sequence will be injected to the MP plant. Given the newest measurements and past N_{mhe}-step of input and measurement data, the constraint MHE (8)-(11) will be incorporated to the system to eliminate the noises on measured states and estimate the unmeasured states. For the MHE, we only consider the case where the model uncertainty ζ_t and measurement noises η_t are normally distributed with zero mean and constant covariance P_ζ and P_η, respectively (6). The detailed algorithm of implementing the simultaneous *m-econ* MPC and MHE is provided in Table 2.

4.2. Simulation Results

We now demonstrate the effectiveness and economical benefits of using the *m-econ* MPC algorithm and MHE in a two-stage HC MP process through simulation examples. To be specific, in the first example, we apply the proposed *m-econ* MPC algorithm with different values of $\sigma \in [0, 1)$ under the assumption that state variables are directly available for the on-line *m-econ* MPC design. Note that with such assumption $\hat{x}_k$ shall be replaced by x_k in previous formulations regarding *m-econ* MPC. From this simulation, we show that the proposed *m-econ* MPC can not only reduce the energy consumption, but also guarantee the closed-loop stability. This algorithm also allows the user to tune the controller in such a way that a desired trade-off between the economic and tracking performances is achieved based on practical demands. In the second example, we provide results for the simultaneous implementation of state estimation and *m-econ* MPC with fixed tuning parameter σ. Moreover, the measurement noise and model uncertainty are considered in the second example.

4.2.1. Example I

In this example, the prediction and control horizons are selected to be equal and set to be $N_{mpc} = 30$. The sampling interval is $2s$, and the simulation length is $T = 160$ samples. The weighting matrices $Q_x = diag\{0.01, 10, 0.1, 10, 0.1\}$ and $Q_u = diag\{0.1, 100, 0.01, 100, 0.01\}$. Note that the tuning parameter σ has to be in the range $[0, 1)$ for the sake of closed-loop stability. However, to more clearly demonstrate the effect of σ on the tracking performance and the economics, here we allow $\sigma = 1$ and will examine the control performance under the following four different values of σ: $\sigma = 0$, $\sigma = 0.5$, $\sigma = 0.75$, and $\sigma = 1$. Note that for $\sigma = 0$, the *m-econ* MPC is reduced to the standard tracking MPC. On the other hand, when $\sigma = 1$, it will be equivalent to *econ* MPC without regulations. $\sigma = 0.5$ and $\sigma = 0.75$ are the two cases where we have the standard *m-econ* MPC. The state estimator will not be considered in this example, thus we assume ζ_k and η_k are zeros in formulation (24)–(29). In the closed-loop simulation, the variations in raw materials such as the chip bulk density d_c and the chip solid content s_c are considered as the disturbances (see Table 3). To address the computational complexity, the nonlinear MP process model is built in AMPL (A Mathematical

[4] Note that model mismatches are not considered in the simulation of the *m-econ* MPC design, otherwise, a static error would persist in presence of non-zero mean disturbances.

Table 3: Variations of d_c and s_c from their nominal values

Time (s)	0-50s	50-110s	110-160s
Chip bulk density (d_c)	80%	115%	90%
Chip solid content (s_c)	90%	100%	110%

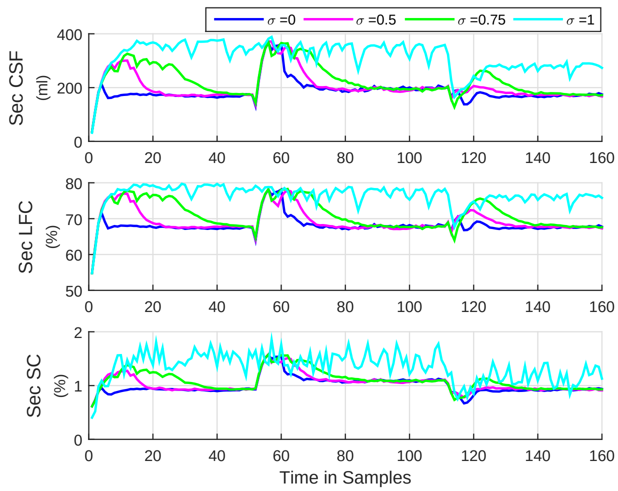

Figure 4: Pulp qualities after secondary HC refining for Example I

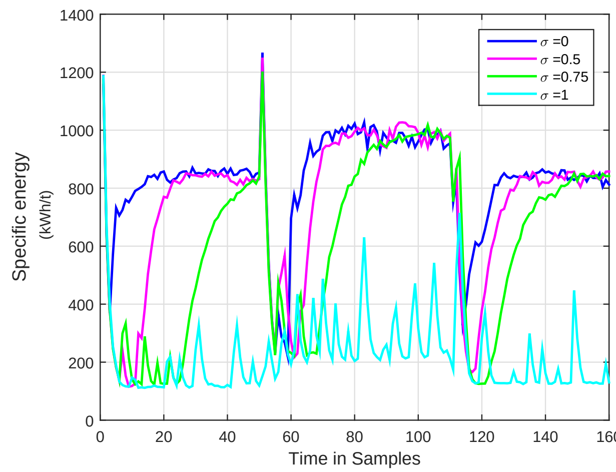

Figure 5: Comparison of the energy reduction for Example I

Programming Language), and the nonlinear optimization problem is solved using IPOPT (Interior Point Optimizer) [34].

The simulation results are shown in Figure 4 – 7. From Figure 4, we can see that for these four situations all pulp qualities after the secondary refining remain within their respective acceptable ranges: $50 - 400$ ml, $50 - 80\%$, and $0 - 2\%$ [5]. However, by using the *econ* MPC ($\sigma = 1$), these pulp qualities are more likely to hit the operating limits compared with the other three MPC schemes. This is obviously not desirable from the perspective of practical operations for mechanical pulping mills. For the case of tracking MPC ($\sigma = 0$), these outputs can rapidly converge to steady-state setpoints. The other two cases can gradually settle down the outputs to steady state with a slower rate compared with tracking MPC. The comparison between the specific energy consumptions of these four situations is illustrated in Figure 5. From Figure 5, one can readily find that the fast convergence speed achieved by tracking MPC is at the price of large energy consumption during the transient stage. Also, the pure *econ* MPC yields the best performance on energy reduction (saves about 73.12% relative to the tracking MPC) possibly because the manipulated variables exert almost all actuations to save energy and thus the resultant tracking performance is the worst according to Figure 4. However, for *m-econ* MPC, it takes account of both the tracking performance and energy reduction. From Figure 5, the *m-econ* MPC with $\sigma = 0.5$ and $\sigma = 0.75$ can save about 10% and 27% of the specific energy,

[5]Detailed nonlinear relationships between state variables and pulp properties can be found in Appendix B.

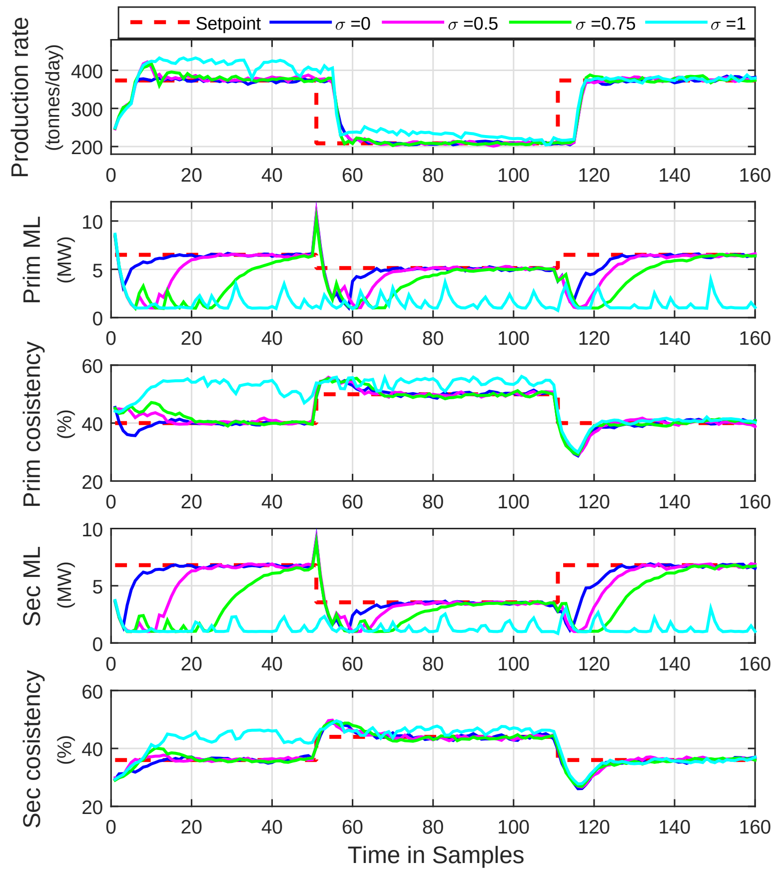

Figure 6: The state variables of the MP process for Example I

Table 4: Energy reduction rate for different σ values of the *m-econ* MPC compared with tracking MPC ($\sigma = 0$)

σ	$\sigma = 0$	$\sigma = 0.5$	$\sigma = 0.75$	$\sigma = 1$
Energy reduction rate	N/A	10%	27%	73%

respectively, compared with the tracking MPC when $\sigma = 0$. Please see Table 4 for detailed energy reduction rate for different σ values of of *m-econ* MPC compared with tracking MPC ($\sigma = 0$).

These conjectures and observations can be more clearly verified by Figure 6 and Figure 7, which illustrate the tracking performance of the state variables and manipulated variables, respectively. It can be seen that for $\sigma = 0$, $\sigma = 0.5$, and $\sigma = 0.75$, the state variables and the manipulated variables converge to the steady-state values but with different convergence speeds. Specifically, as σ decreases, the tracking speed of *m-econ* MPC improves, which is consistent with our analysis since smaller σ values imply more emphasis on the tracking performance. For the extreme case where $\sigma = 1$, the convergence and stability cannot be guaranteed since the target in this case will be merely achieving the optimal economic performance regardless of the tracking performance or even the stability.

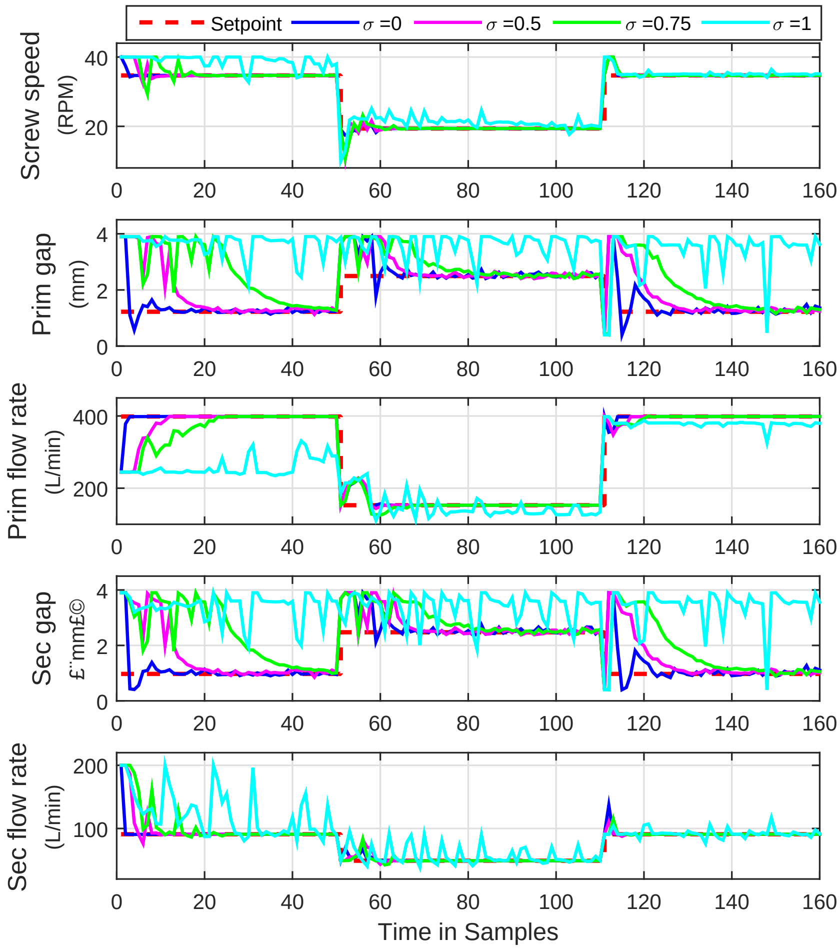

Figure 7: The manipulated variables of the MP process for Example I

4.2.2. Example II

In this example, the MHE is incorporated in the two-stage refining system as part of the feedback control of the *m-econ* MPC. The model uncertainty and measurement noise are considered in the closed-loop simulation. The measured (but noisy) state variables in the HC MP process are production rate, primary motor load and secondary motor load. The unmeasured state variables, which are the consistencies for the primary and secondary refiners, are estimated by MHE from the noisy measurements and past input data. In this example, the simulation duration is $T = 450$ samples. The estimation horizon $N_{mhe} = 15$ with arrival cost weighting vector selected to be $\mu = [0.5, 1, 0.1]$. It is assumed that the simulation and real MP process share the same disturbance and measurement noise covariance $P_\zeta = [1, 0.1, 1, 0.1, 0.5]$, $P_\eta = [0.1, 0.1, 0.1, 0.1, 0.1]$, respectively. The tuning parameter σ is fixed and chosen to be 0.8. The other parameters are set the same as those in the previous simulation. Note that in this example the computational time by using IPOPT is fast enough to ensure that both MHE and *m-econ* MPC can be solved within each sampling interval.

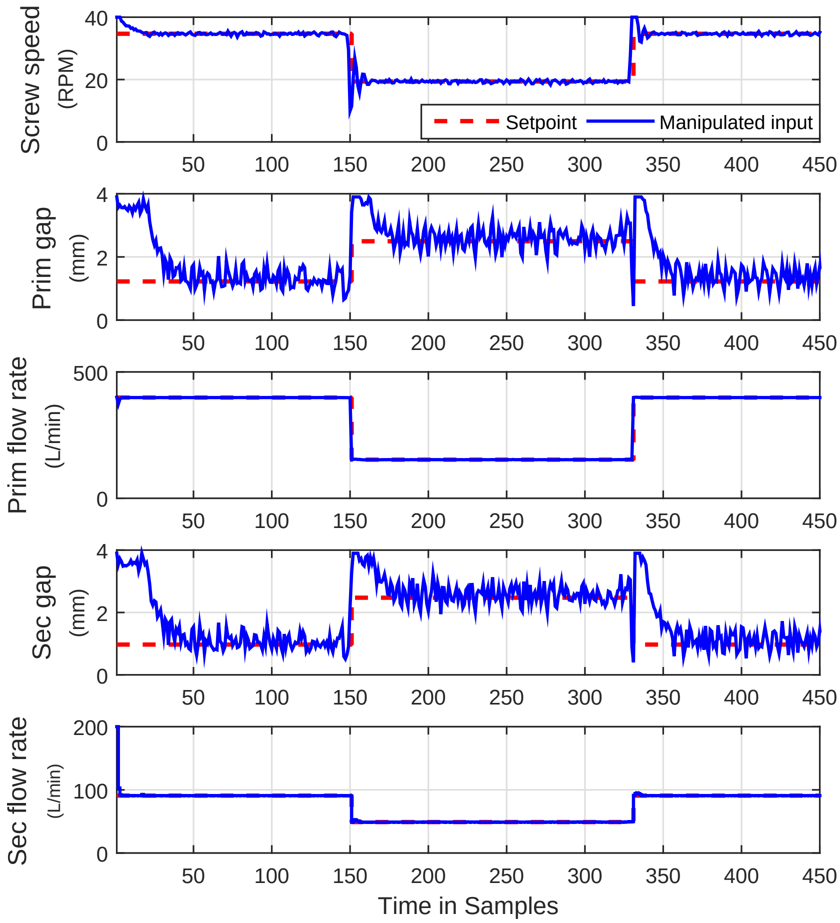

Figure 8: The manipulated variables of the MP process for Example II

The simulation results are shown in Figure 8 − 10. The manipulated variables for the closed-loop two-stage HC refining process are given in Figure 8. From Figure 8, we can find that all manipulated variables in the two-stage HC process are able to track the setpoints within 50 samples. Besides, the output variables, which are actually states x_1, x_2 and x_3 (plus noise), can approach the respective setpoints quickly under the proposed integrated MHE and *m-econ* MPC framework. The tracking performance of all five states are illustrated in Figure 9. It is apparent from Figure 9 that MHE can yield precise estimates for both measured and unmeasured states, which is evidenced by the large overlapping between the actual and estimates states. The specific energy consumption in this example is shown in Figure 10, and the energy saving rate with $\sigma = 0.8$ is about 30% compared with the tracking MPC from the previous example.

5. Conclusion

This paper presents an integrated framework consisting of *m-econ* MPC and MHE for a nonlinear two-stage HC MP process. The *m-econ* MPC inherits the merits of economic MPC in reducing energy consumption and that of *tr* MPC in ensuring the closed-loop stability. It is shown that the *m-econ* MPC enables the user

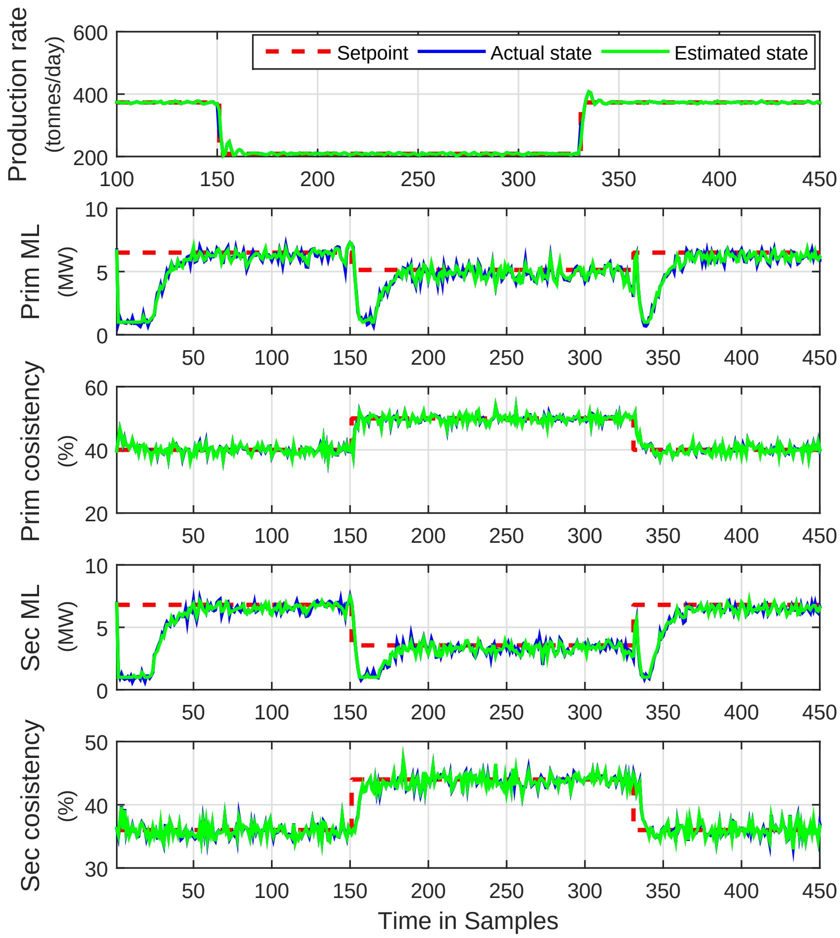

Figure 9: The state variables of the MP process for Example II

to make an informed trade-off between production economics and the convergence speed of process variables to the setpoints. For industrial processes with unmeasured states, including the MP processes, we propose to combine online MHE together with the *m-econ* MPC into an integrated framework that can be implemented in practice. Two simulation examples from MP processes are provided to demonstrate the advantages of using *m-econ* MPC and the effectiveness of the entire *m-econ* MPC and MHE scheme.

6. ACKNOWLEDGMENTS

This work was supported by the Natural Sciences and Engineering Research Council of Canada through the Collaborative Research and Development program and through the support of our partners: AB Enzymes, Alberta Newsprint Company, Andritz, BC Hydro, Canfor, Catalyst Paper, FPInnovations, Holmen Paper, Millar Western, NORPAC, Paper Excellence, Quesnel River Pulp, Slave Lake Pulp, Westcan Engineering, and Winstone Pulp International. Our special thanks goes to Alberta Newsprint, FPInnovations, and Howe Sound Pulp and Paper (Paper Excellence) for providing data for our models. Victor M. Zavala acknowledges support from the members of the TWCCC consortium.

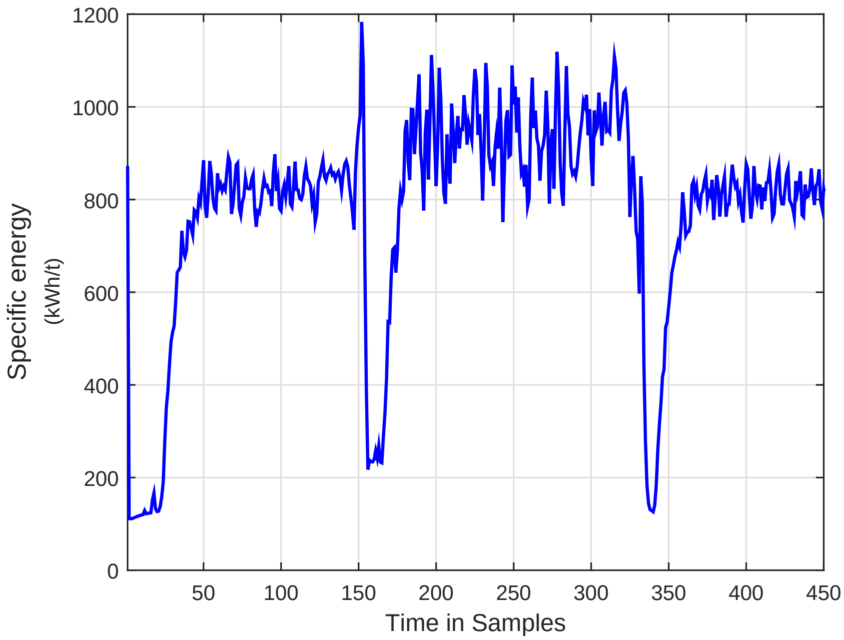

Figure 10: Specific energy for Example II

Appendix A. Two-stage HC MP Process Model

MP processes are inherently MIMO processes with complex dynamics and interactions among process variables. Modeling of MP process is challenging due to the complex mechanism inside of the pulp refiners. In this section, the two-stage HC MP process model is presented. The mathematical model is developed by using a combination of mechanistic and empirical methods, which will not only give some insights into mechanism, interactions, and nonlinearity of the MP refining process, but also characterize the feature of MP process dynamics. In this paper, the following process variables are used to develop a discrete-time nonlinear model for the MP process [20, 27].

Production rate

$$P = k_a \cdot k_p \cdot s_c \cdot d_c \cdot R, \tag{A.1}$$

where P $(tonnes/day)$ is the production rate. k_a and k_p (m^3/rev) are constant parameters which can be obtained from the industrial data and their values depend on the particular production lines. $s_c(\%)$ is the chip solid content. d_c (kg/m^3) is the chip bulk density. R (rpm) is the chip-transfer screw speed.

Motor load

$$M_i = \frac{k_{m_i} \cdot P}{D_i}(1 - e^{(-10G_i)})(c_i - e_i \cdot G_i), \quad i = p, s, \tag{A.2}$$

where M_i (MW) is the motor load for the i-th refiner, $i = p, s$. D_i (l/min) is the dilution water flow rate. G_i (mm) is the gap distance. c_i, e_i, and k_{m_i} are the parameters of each refiner.

Consistency

$$C_p = \frac{100P}{P + k_a \cdot D_p - k_{e_p} \cdot M_p}, \tag{A.3}$$

$$C_s = \frac{100P}{P/(0.01C_p) + k_a \cdot D_s - k_{e_s} \cdot M_s}, \tag{A.4}$$

where C_p and C_s are the consistency for the primary and secondary refiner, respectively. k_a, k_{e_p} and k_{e_s} are the refiner parameters.

By introducing linear dynamics for the discretized differential state variables and superimposing it on the steady-state relationships (A.1)–(A.4), a Wiener type discrete-time nonlinear model for the MP process can be formulated at sample time t as in (3)–(4) with the state variables and manipulated input variables defined in Table 1. One can use the time constant and time delay information of each subprocesses to form the dynamic matrix A as follows [35],

$$\bar{A}(z) = \begin{pmatrix} g_1(z) & 0 & 0 & 0 & 0 \\ 0 & g_2(z) & 0 & 0 & 0 \\ 0 & 0 & g_3(z) & 0 & 0 \\ 0 & 0 & 0 & g_4(z) & 0 \\ 0 & 0 & 0 & 0 & g_5(z) \end{pmatrix}, \tag{A.5}$$

where $\bar{A}(z)$ is the dynamic transfer function matrix of the MP process. $g_1(z)$ is the transfer function between the production rate and the chip-transfer screw speed. $g_2(z)$ is the transfer function between the primary motor load and the primary refiner gap. $g_3(z)$ is the transfer function between the primary consistency and the primary dilution flow rate. $g_4(z)$ is the transfer function between the secondary refiner motor load and the secondary refiner plate gap. $g_5(z)$ is the transfer function between the secondary consistency and the secondary dilution flow rate. The transfer functions $g_i(z), i = 1, \cdots, 5$ have the following forms,

$$g_i(z) = \frac{b_i z^{-d_i}}{z - a_i}, \quad , i = 1, \cdots, 5, \tag{A.6}$$

where a_i and d_i, $i = 1, \cdots, 5$, are the poles and time delays of the subprocess, respectively. $b_i = 1 - a_i$, $i = 1, \cdots, 5$, are parameters for unity dynamic gains of each subprocess. Note that the parameters a_i, d_i, and b_i will vary with the different refiners in each pulp mill. Then the dynamic matrix can be expressed as,

$$A = diag\{a_1, a_2, a_3, a_4, a_5\}. \tag{A.7}$$

The nonlinear state function $h(\cdot) : \mathbb{R}^{n_x} \times \mathbb{R}^{n_u} \mapsto \mathbb{R}^{n_x}$ in (3) is then defined as $h = (I - A)H$, where H maps steady-state control input variables to steady-state differential state variables of the MP process model.

By superimposing the nonlinear steady-state functions (A.1)–(A.4) to the linear dynamics of the two-stage HC MP process (A.5)–(A.7), the nonlinear two-stage HC MP process can be described as follows,

$$x_{t+1}^1 = a_1 x_t^1 + b_1 k_a \cdot k_p \cdot s_c \cdot d_c \cdot u_t^1, \tag{A.8}$$

$$x_{t+1}^2 = a_2 x_t^2 + b_2 \frac{k_{m_1} \cdot x_t^1}{u_t^3}(1 - e^{(-10u_t^2)})(c_1 - e_1 \cdot u_t^3), \tag{A.9}$$

$$x_{t+1}^3 = a_3 x_t^3 + b_3 \frac{100 x_t^1}{x_t^1 + k_a \cdot u_t^3 - k_{e_p} \cdot x_t^2}, \tag{A.10}$$

$$x_{t+1}^4 = a_4 x_t^4 + b_4 \frac{k_{m_2} \cdot x_t^1}{u_t^5}(1 - e^{(-10u_4^t)})(c_2 - e_2 \cdot u_4^t), \tag{A.11}$$

$$x_{t+1}^5 = a_5 x_t^5 + b_5 \frac{100 x_t^1}{x_t^1/(0.01 x_t^3) + k_a \cdot u_t^5 - k_{e_s} \cdot x_t^4}. \tag{A.12}$$

where the notation x_t^i, u_t^i, $i = 1, \cdots, 5$, are the i-th state or manipulated variables (defined in Table 1) at sampling time t, respectively.

Appendix B. Pulp quality modeling

In this work, we use the nonlinear model developed in [5, 11] to predict the pulp properties of CSF, LFC, and SC. The following declinations are introduced before we establish the nonlinear pulp property models.

Refining intensity

The refining intensity (RI) has been suggested as an important variable in all types of refining [15]. For a given SE, different RI will produce the pulp with quite different quality.

$$RI_i = \frac{SE_i}{N_i}, \quad i = p, s, \tag{B.1}$$

where SE_i is the specific energy as defined in (1). N_i is the total number of impacts and is given by,

$$N_i = n_i h_i \omega_i [(r_{1i} + r_{2i})/2] \tau_i, \quad i = p, s, \tag{B.2}$$

where n_i is the number of bars per unit length of arc of a refiner disc. $h_i = 1$ for a single disc refiner, and $h_i = 2$ for a double disc refiner. $\omega_i (radians/s)$ is the refiner rotational speed. r_{1i}, $r_{2i}(m)$ are the inlet and outlet radius of plates' refining zone. $\tau_i(s)$ is the residence time of the wood chips in the i-th refiner.

Specific refining power

The specific refining power (SRP) describes the energy-transfer rate. For the i-th refiner, it is defined as,

$$SRP_i = \frac{SE_i}{\tau_i}, \quad i = p, s \tag{B.3}$$

The empirical relationships between pulp properties of CSF, LFC, and SC and the intermediate variables SE_i, RI_i, and SRP_i can be expressed as [11],

$$CSF_i = [CSF_{i0} - k_i^{csf_1}(SE_i - SE_{i0})] \cdot 10^{-k_i^{csf_2}(RI_i - RI_{i0})}, \tag{B.4}$$

$$LFC_i = LFC_{i0} - k_i^{lfc_1}(SRP_i - SRP_{i0}) - k_i^{lfc_2}(SE_i - SE_{i0}), \tag{B.5}$$

$$SC_i = SC_{i0} \cdot 10^{-[k_i^{sc_1}(SE_i - SE_{i0}) + K_i^{sc_2}(SRP_i - SRP_{i0})]}, \quad i = p, s \tag{B.6}$$

where CSF_{i0}, LFC_{i0}, and SC_{i0} are the initial values of pulp properties. SE_{i0}, RI_{i0}, and SRP_{i0} are the initial values of the SE_i, RI_i, and SRP_i, respectively. $k_i^{csf_1}$, $k_i^{csf_2}$, $k_i^{lfc_1}$, $k_i^{lfc_2}$, $k_i^{sc_1}$, and $k_i^{sc_2}$ are parameters of the primary and secondary refiners and may vary with the different refiners in each pulp mills .

References

[1] G. A. Dumont, Application of advanced control methods in the pulp and paper industry – a survey, Automatica, 22 (2) (1986) 143–153.

[2] D. Chruch, Current and projected pulp and paper industry problems in process control and process modelling, AiChE Symp. Series, 72 (8) (1976) 19–39.

[3] D. D. Ruscio, Topics in model based control with application to the thermo mechanical pulping process, Ph.D. thesis, The Norwegian Institute of Technology, Norway (1993).

[4] B. J. Allison, J. E. Ciarniello, P. J. C. Tessier, G. A. Dumont, Dual adaptive control of chip refiner motor load, Automatica, 31 (8) (1995) 1169–1184.

[5] X. Qian, P. Tessier, A mechanistic model for predicting pulp properties from refiner operating conditions, Tappi Journal, 78 (78) (1995) 215–222.

[6] A. Luukkonen, J. A. Olson, D. M. Martinez, Low consistency refining of mechanical pulp: Effect of gap, speed, and power, Journal of Pulp and Paper Science, 36 (1–2) (2010) 28–34.

[7] D. J. Marshman, T. Chmelyk, M. S. Sidhu, R. B. Gopaluni, G. A. Dumont, Energy optimization in a pulp and paper mill cogeneration facility, Applied Energy, 87 (11) (2010) 3514–3525.

[8] A. Luukkonen, J. A. Olson, D. M. Martinez, Low consistency refining of mechanical pulp: A methodology to relate operating conditions to paper properties, Journal of Pulp and Paper Science, 36 (3–4) (2010) 107–111.

[9] E. Harinath, L. T. Biegler, G. A. Dumont, Advanced step nonlinear model predictive control for two-stage thermo mechanical pulping processes, IFAC Proceedings Volumes, 44 (1) (2011) 3653–3658.

[10] E. Harinath, L. T. Biegler, G. A. Dumont, Control and optimization strategies for thermo-mechanical pulping processes: Nonlinear model predictive control, Journal of Process Control, 21 (4) (2011) 519–528.

[11] E. Harinath, L. T. Biegler, G. A. Dumont, Predictive optimal control for thermo-mechanical pulping processes with multi-stage low consistency refining, Journal of Process Control, 23 (7) (2013) 1001–1011.

[12] S. J. Qin, T. A. Thomas, A survey of industrial model predictive control technology, Control Engineering Practice, 11 (7) (2003) 733–764.

[13] L. Wang, Model Predictive Control System Design and Implementation Using MATLAB, Springer Science & Business Media, 2009.

[14] E. F. Camacho, C. Bordons, Model Predictive Control, Springer Science & Business Media, 2013.

[15] H. Du, Multivariable predictive control of a tmp plant, Ph.D. thesis, University of British Columbia, Canada (1998).

[16] B. Kouvaritakis, M. Cannon, Non-linear Predictive Control: Theory and Practice, The Institution of Engineering and Technology, London, 2001.

[17] D. Limon, M. Pereira, D. M. De La Peña, T. Alamo, J. M. Grosso, Single-layer economic model predictive control for periodic operation, Journal of Process Control, 24 (8) (2014) 1207–1224.

[18] L. N. Petersen, J. B. Jørgensen, J. B. Rawlings, Economic optimization of spray dryer operation using nonlinear model predictive control with state estimation, The 9th International Symposium on Advanced Control of Chemical Processes, (2015) 507–513.

[19] H. Durand, M. Ellis, P. D. Christofides, Accounting for the control actuator layer in economic model predictive control of nonlinear processes, American Control Conference, (2015) 2968–2973.

[20] H. Tian, Q. Lu, R. B. Gopaluni, V. M. Zavala, Multi-objective economic mpc of mechanical pulping processes, Proceedings of the 55th IEEE Conference on Decision and Control, (2016) 4040–4045.

[21] D. W. Griffith, V. M. Zavala, L. T. Biegler, Robustly stable economic nmpc for non-dissipative stage costs, Journal of Process Control, 57 (2017) 116–126.

[22] C. V. Rao, J. B. Rawlings, Nonlinear moving horizon state estimation, In Nonlinear Model Predictive Control, Basel: Birkhäuser, 2000.

[23] P. E. Moraal, J. W. Grizzles, Observer design for nonlinear systems with discrete-time measurements, IEEE Transactions on Automatic Control, 40 (3) (1995) 395–404.

[24] H. Michalska, D. W. Mayne, Moving horizon observers and observer-based control, IEEE Transactions on Automatic Control, 40 (6) (1995) 995–1000.

[25] C. V. Rao, J. B. Rawlings, D. W. Mayne, Constrained state estimation for nonlinear discrete-time systems: Stability and moving horizon approximations, IEEE Transactions on Automatic Control, 42 (2) (2003) 246–258.

[26] A. Alessandri, M. Baglietto, G. Battistelli, Moving-horizon state estimation for nonlinear discrete-time systems: New stability results and approximation schemes, Automatica, 44 (72) (2008) 1753–1765.

[27] H. Tian, Q. Lu, R. B. Gopaluni, V. M. Zavala, J. A. Olson, Economic nonlinear model predictive control for mechanical pulping processes, American Control Conference, (2016) 1796–1801.

[28] V. M. Zavala, Stability analysis of an approximate scheme for moving horizon estimation, Computers & Chemical Engineering, 34 (10) (2010) 1662–1670.

[29] R. Huang, E. Harinath, L. T. Biegler, Lyapunov stability of economically oriented nmpc for cyclic processes, Journal of Process Control, 21 (4) (2011) 501–509.

[30] M. Diehl, R. Amrit, J. B. Rawlings, A lyapunov function for economic optimizing model predictive control, IEEE Transactions on Automatic Control, 56 (3) (2011) 703–707.

[31] D. Angeli, R. Amrit, J. B. Rawlings, On average performance and stability of economic model predictive control, IEEE Transactions on Automatic Control, 57 (7) (2012) 1615–1626.

[32] D. Q. Mayne, J. B. Rawlings, C. V. Rao, P. O. Scokaert, Constrained model predictive control: Stability and optimality, Automatica, 36 (6) (2000) 789–814.

[33] V. M. Zavala, A multiobjective optimization perspective on the stability of economic mpc, IFAC-PapersOnLine, 48 (8) (2015) 975–981.

[34] A. Wächter, L. T. Biegler, On the implementation of an interior-point filter line-search algorithm for large-scale nonlinear programming, Mathematical Programming, 106 (1) (2006) 25–57.

[35] E. Harinath, Identification, control and optimization strategies for thermo-mechanical pulping (tmp) processes, Ph.D. thesis, University of British Columbia, Canada (2012).